

This is an Open Access document downloaded from ORCA, Cardiff University's institutional repository: <https://orca.cardiff.ac.uk/id/eprint/149432/>

This is the author's version of a work that was submitted to / accepted for publication.

Citation for final published version:

Zheng, Gangfeng, Azorin-Molina, Cesar, Wang, Xuejia, Chen, Deliang, McVicar, Tim R., Guijarro, Jose A., Chappell, Adrian, Deng, Kaiqiang, Minola, Lorenzo, Kong, Feng, Wang, Shuo and Shi, Peijun 2022. Rapid urbanization induced daily maximum wind speed decline in metropolitan areas: a case study in the Yangtze River Delta (China). *Urban Climate* 43, 101147. 10.1016/j.uclim.2022.101147

Publishers page: <https://doi.org/10.1016/j.uclim.2022.101147>

Please note:

Changes made as a result of publishing processes such as copy-editing, formatting and page numbers may not be reflected in this version. For the definitive version of this publication, please refer to the published source. You are advised to consult the publisher's version if you wish to cite this paper.

This version is being made available in accordance with publisher policies. See <http://orca.cf.ac.uk/policies.html> for usage policies. Copyright and moral rights for publications made available in ORCA are retained by the copyright holders.



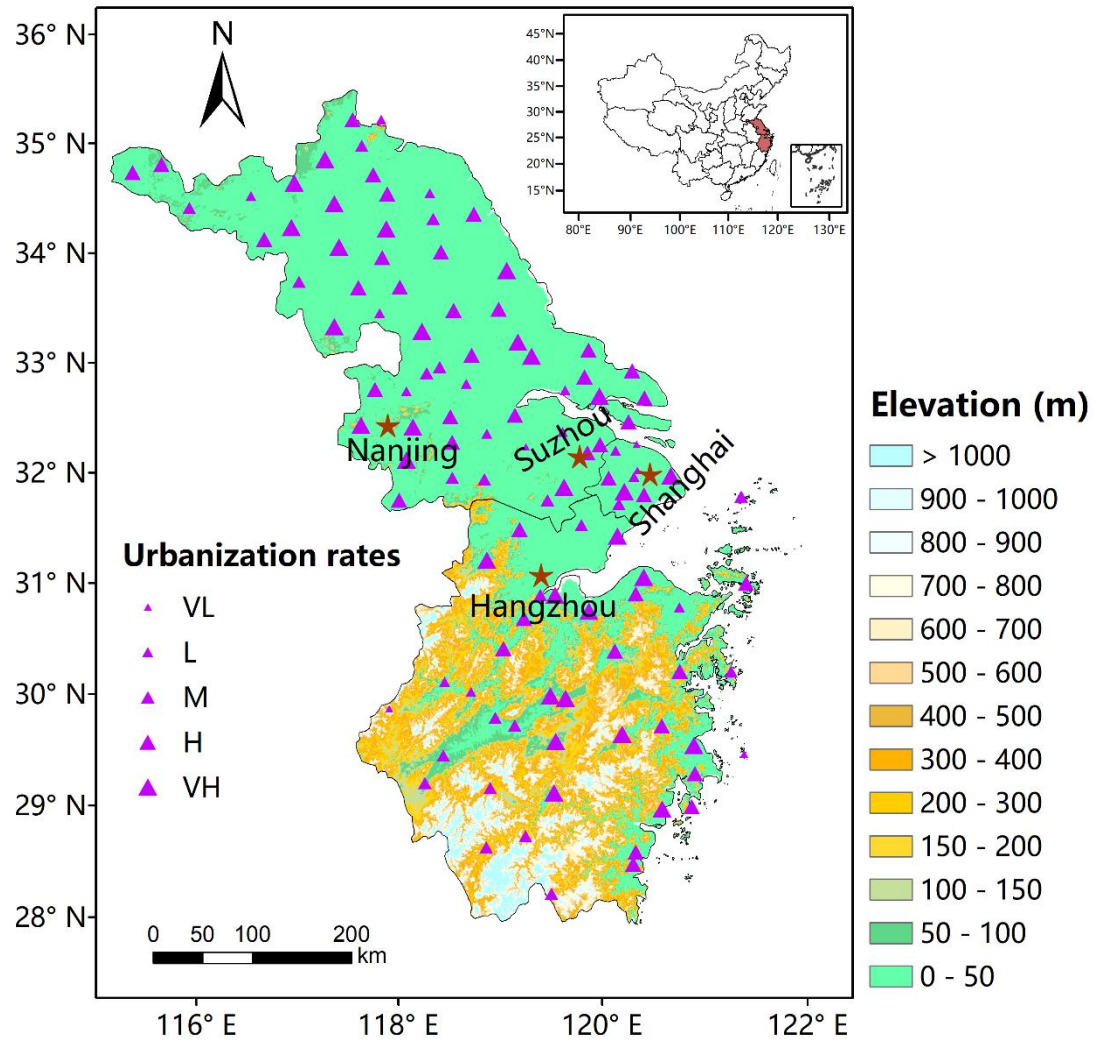


Figure 1. Distribution of the 111 homogenized stations recording DMWS, and terrain over the Yangtze River Delta. Names of the four largest cities are also displayed in the map. The inset map shows the location of the Yangtze River Delta in China. The size of triangle represents the five urbanization rates at each station: VL (very low), L (low), M (moderate), H (high), and VH (very high).

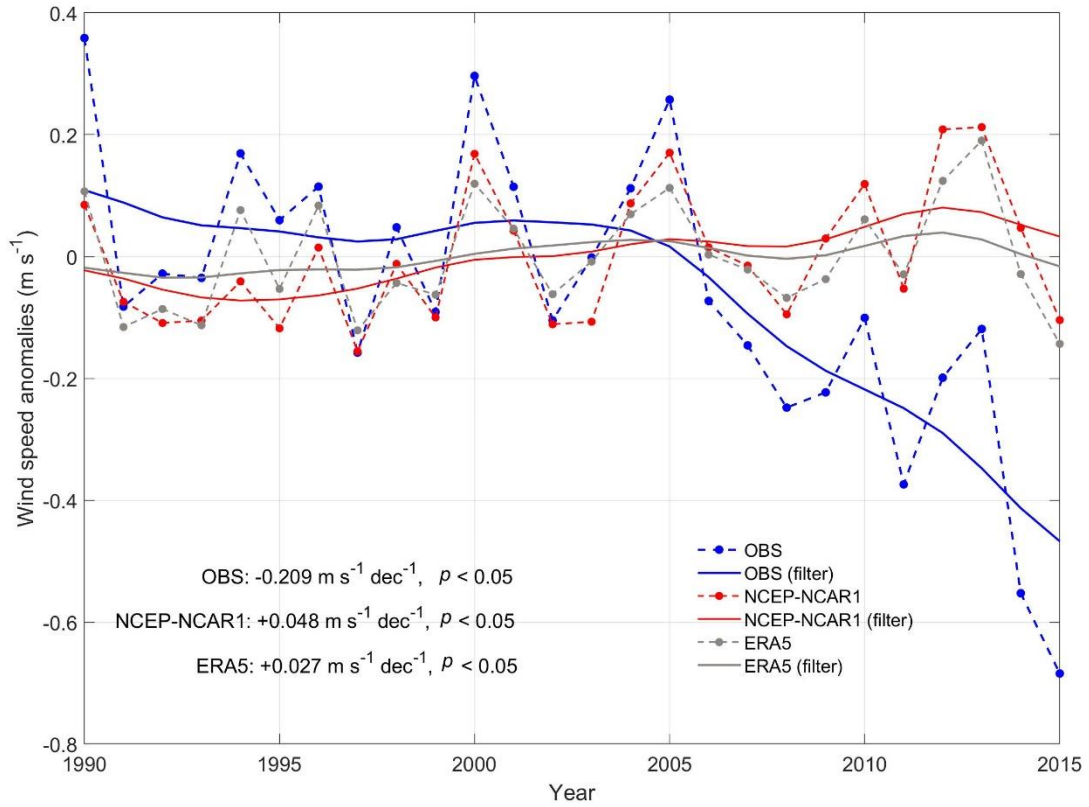


Figure 2. Variability of Daily Maximum Wind Speed (DMWS) anomaly from station observations (OBS) during 1990–2015 over the Yangtze River Delta. DMWS from 6 hourly NCEP-NCAR1 wind speed and hourly ERA5 wind speed are also displayed. Wind speed anomalies at each station and grid (in m s^{-1}) are calculated as the deviation from the 1990–2015 mean, and the regional mean annual anomalies were then calculated as shown here. A solid line indicates the 11-year Gaussian low-pass filter. The magnitude (in $\text{m s}^{-1} \text{ dec}^{-1}$) and statistical significance (p -level) of the regional (Mann–Kendall’s tau-b non-parametric) trends were also displayed for each of the three data sources.

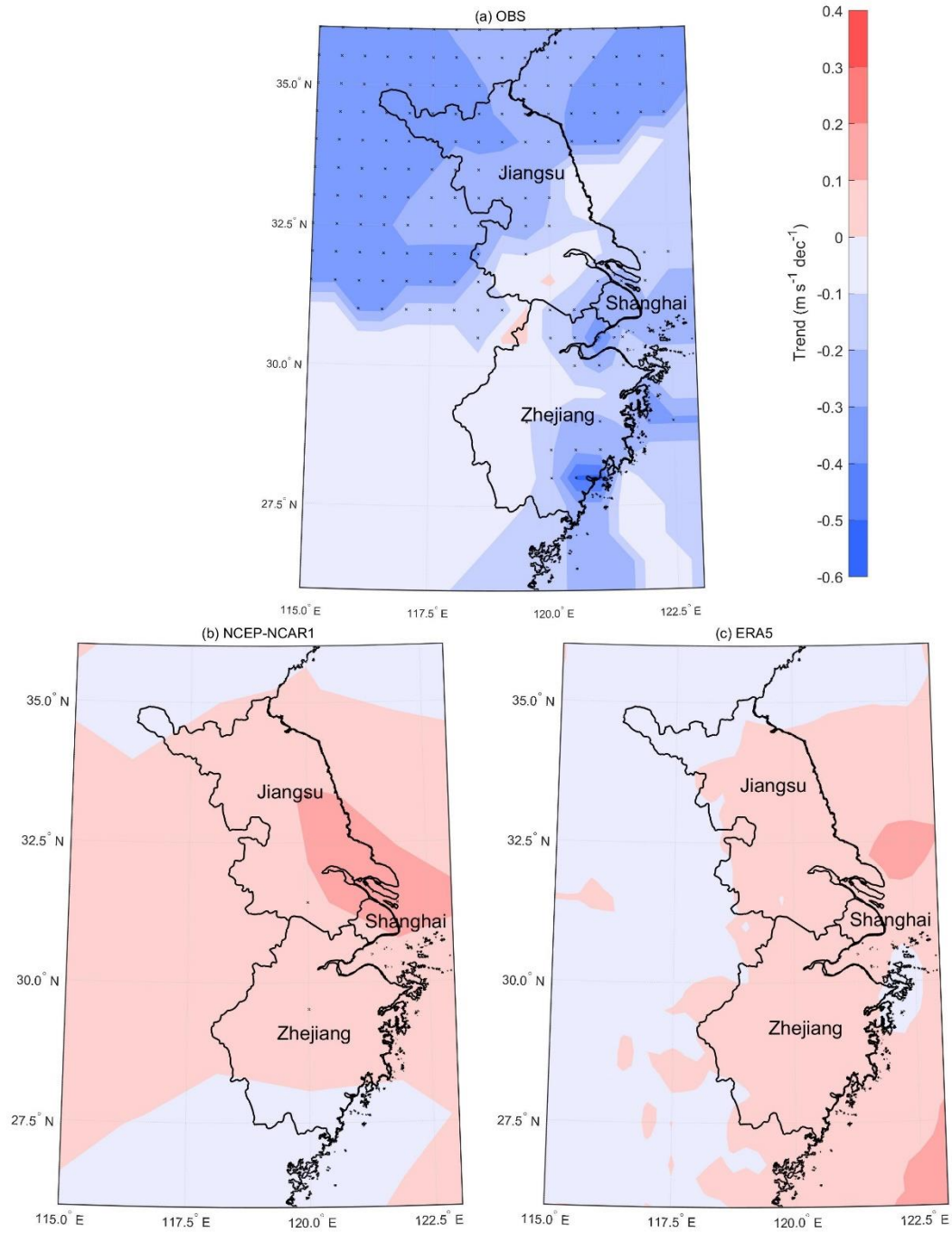


Figure 3. Spatial distribution of annual Daily Maximum Wind Speed (DMWS) trends (in $\text{m s}^{-1} \text{dec}^{-1}$) from (a) station observations (OBS), (b) NCEP-NCAR1, and (c) ERA5 for 1990-2015 over the Yangtze River Delta. Names of the three sub-regions are also displayed in the map. The black dot in the grid represents a statistically significant trend at $p < 0.05$. The legend in the upper right applies to all parts. Internal black lines are province boundaries

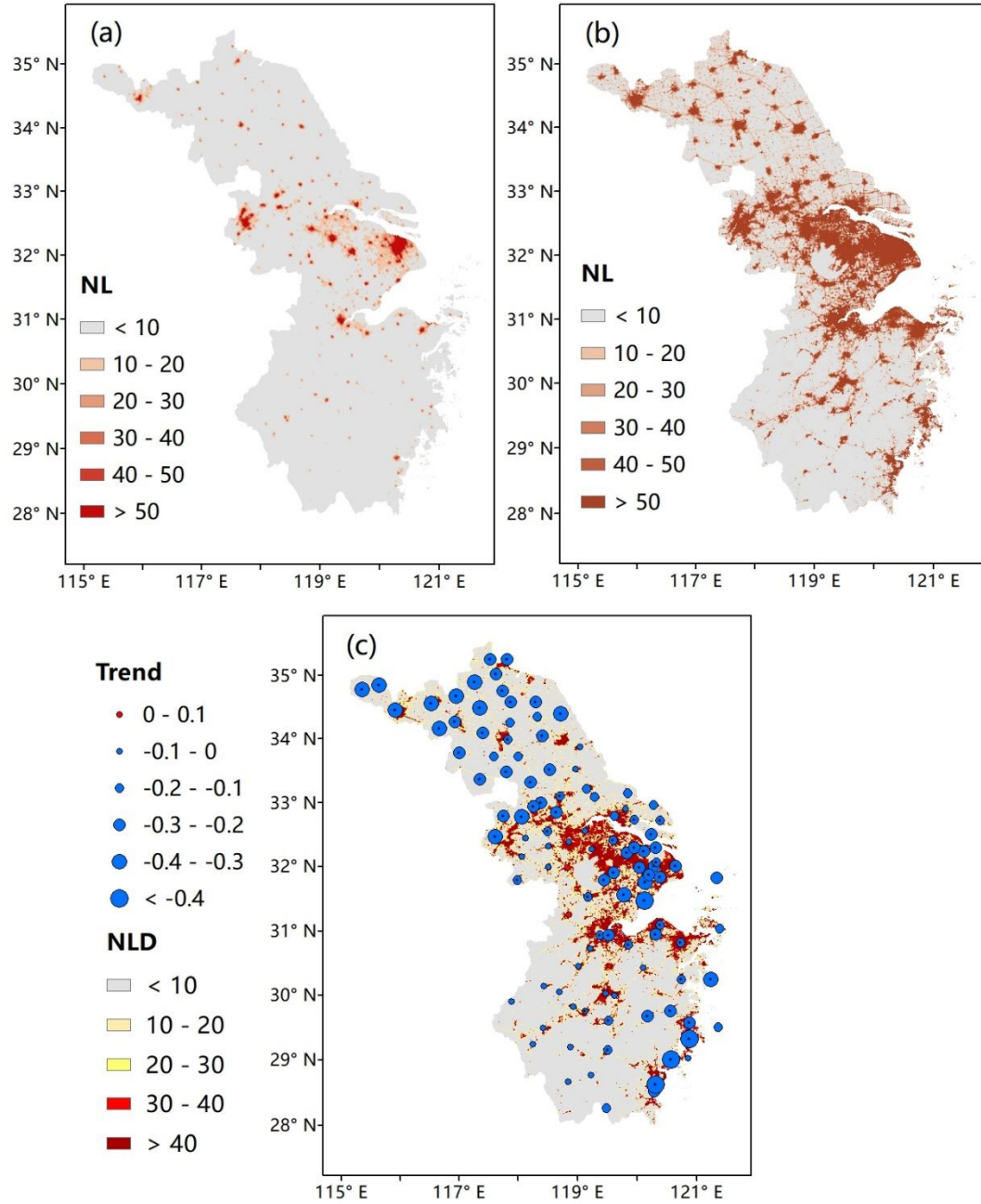


Figure 4. Distribution of night-time light (NL, dimensionless) in (a) 1992 and (b) 2015 in the Yangtze River Delta, and (c) night-time light difference (NLD, dimensionless) between 2015 and 1992 (2015 minus 1992). For the comparison with NLD, trends (in $\text{m s}^{-1} \text{dec}^{-1}$) as well as associated significance of Daily Maximum Wind Speed (DMWS) for 1990-2015 in each of the 111 stations are also displayed in the map. A black dot in the blue circle represents a significant trend at $p < 0.05$. The lower left legend is only for (c).

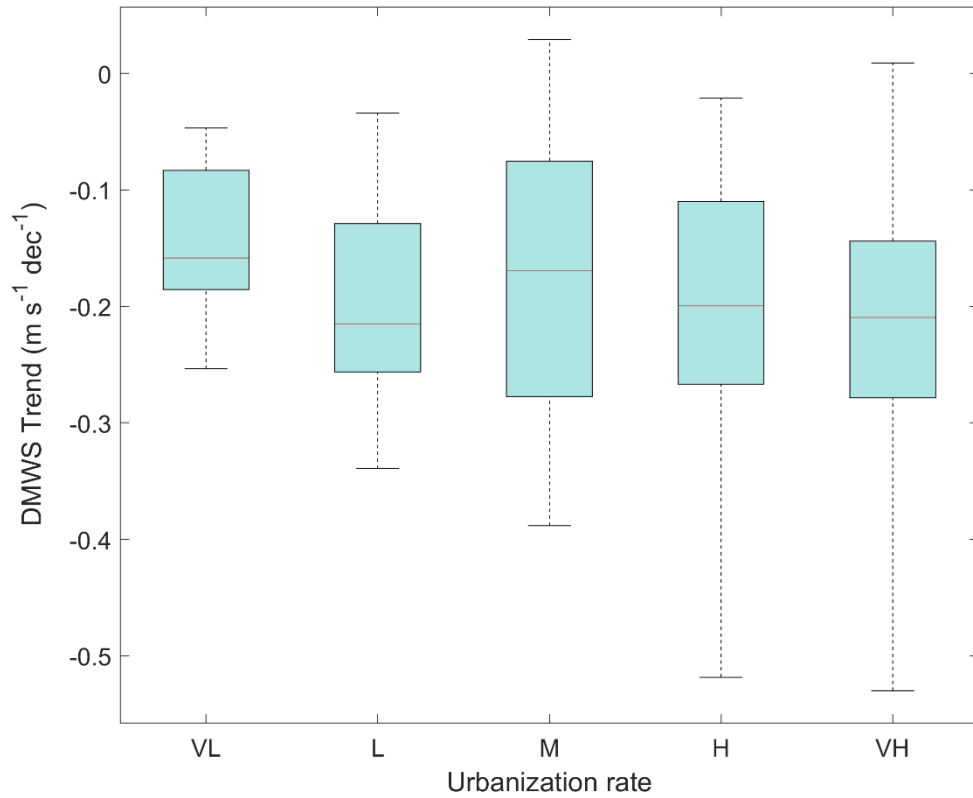


Figure 5. Box-and-whisker plots of Daily Maximum Wind Speed (DMWS) trends in different station categories with varying urbanization rates across the Yangtze River Delta from 1990 to 2015. The median (red line), the 25th and 75th percentile range (boxes), and the 10th and 90th percentiles (whiskers) for each station category are provided. The horizontal axis represents five urbanization rates: VL (very low), L (low), M (moderate), H (high), and VH (very high).

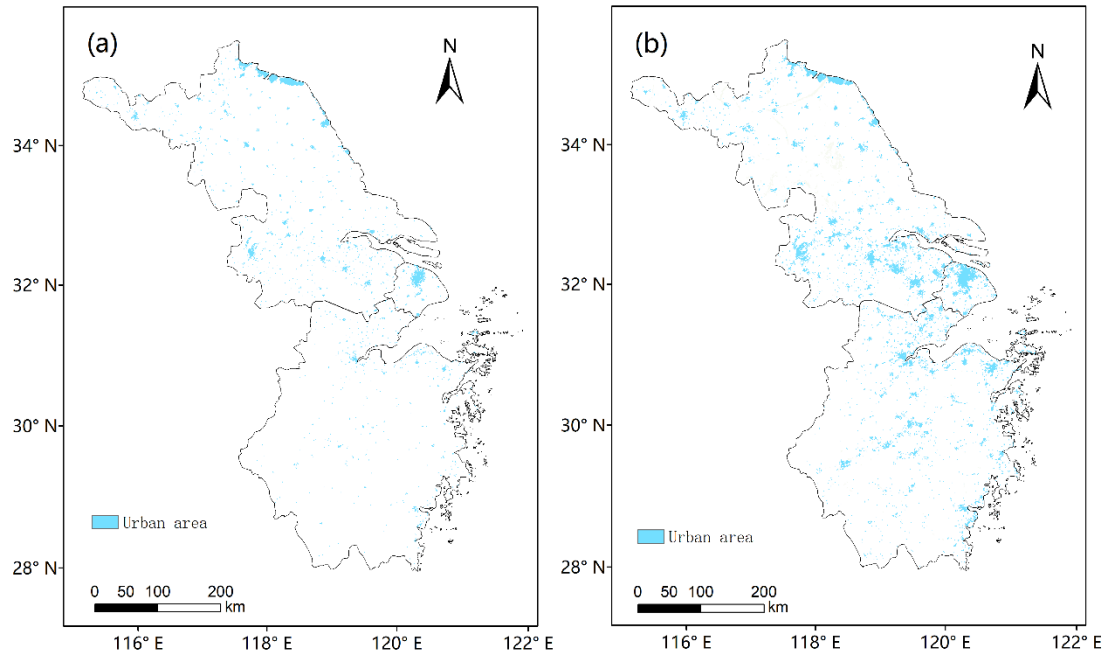


Figure 6. Distribution of urban areas (blue) in (a) 1990 and (b) 2015 in the Yangtze River Delta. Internal black lines are province boundaries.

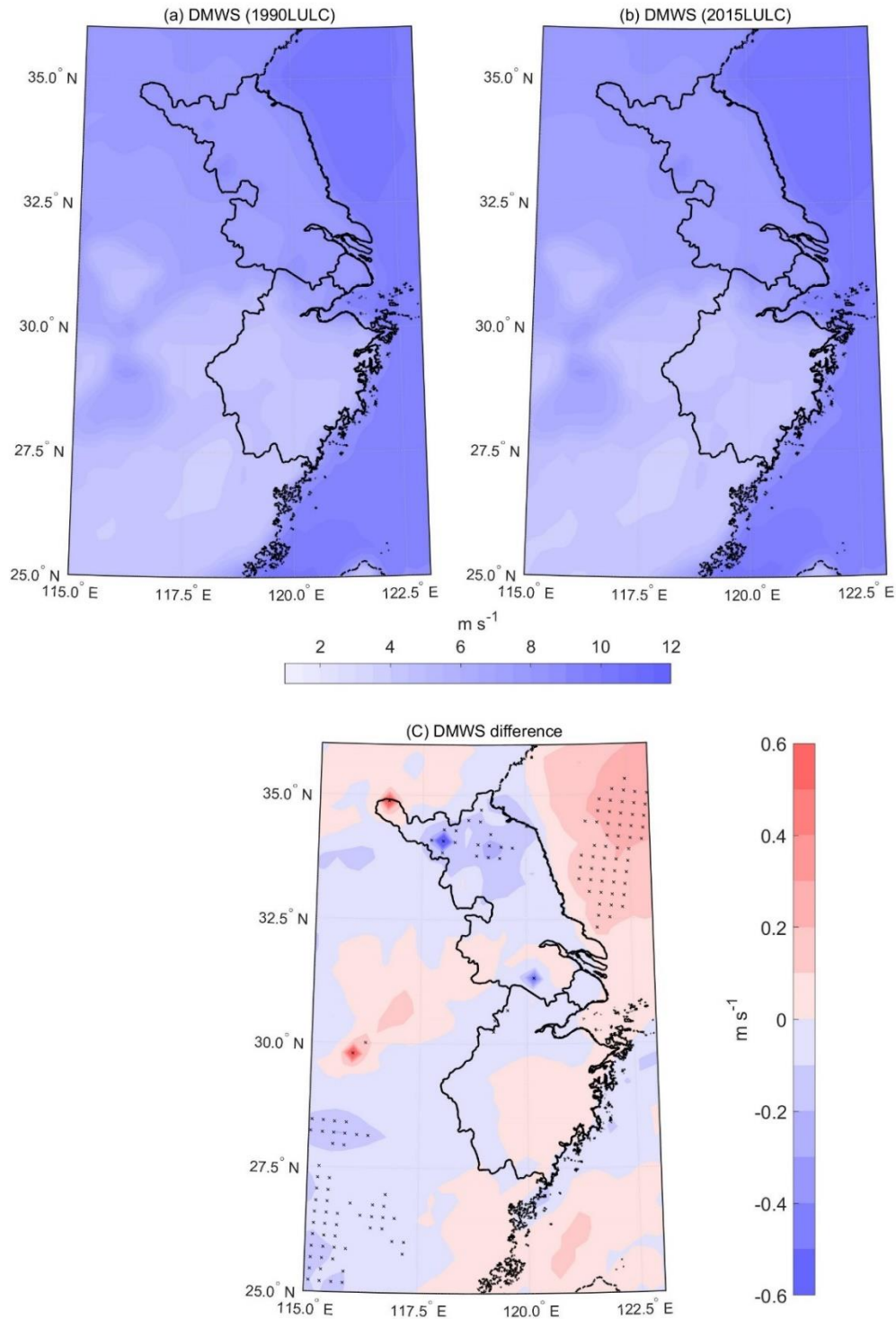


Figure.7 Spatial pattern of Daily Maximum Wind Speed (DMWS) in model simulations under different land use and land cover (1990LULC and 2015LULC) data but with the same other settings and forcing. Also shown is the DMWS difference between the two simulations. (a) DMWS for 1990 using 1990LULC data, (b) DMWS for 1990 using 2015LULC data, and (c) DMWS difference (calculated as (b)-(a)). Note that horizontal legend is used for (a) and (b), and the vertical legend for (c). The black dot in the grid represents a statistically significant DMWS difference at $p < 0.1$. Internal black lines are province boundaries.

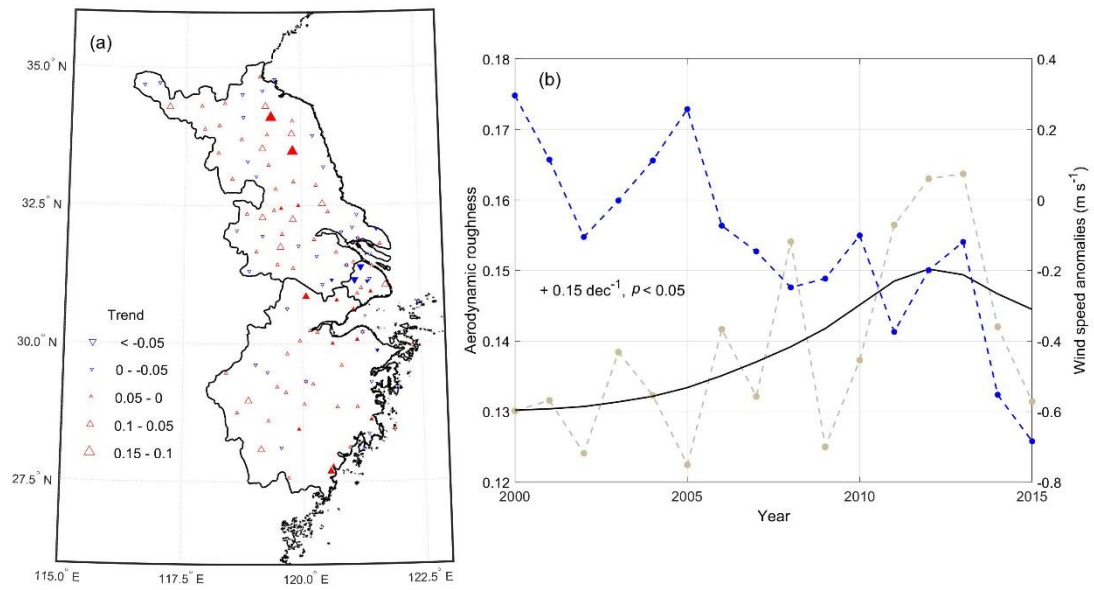


Figure 8. (a) Distribution of annual mean aerodynamic roughness (unitless) trends (dec^{-1}) at each station from 1990 to 2015. Statistically insignificant trends ($p > 0.05$) are represented by unfilled symbols. (b) Variability of the annual mean aerodynamic roughness of all the stations over the Yangtze River Delta from 2000 to 2015, as well as the trend and statistical significance. Note station observed DMWS is displayed in right Y-axis label.

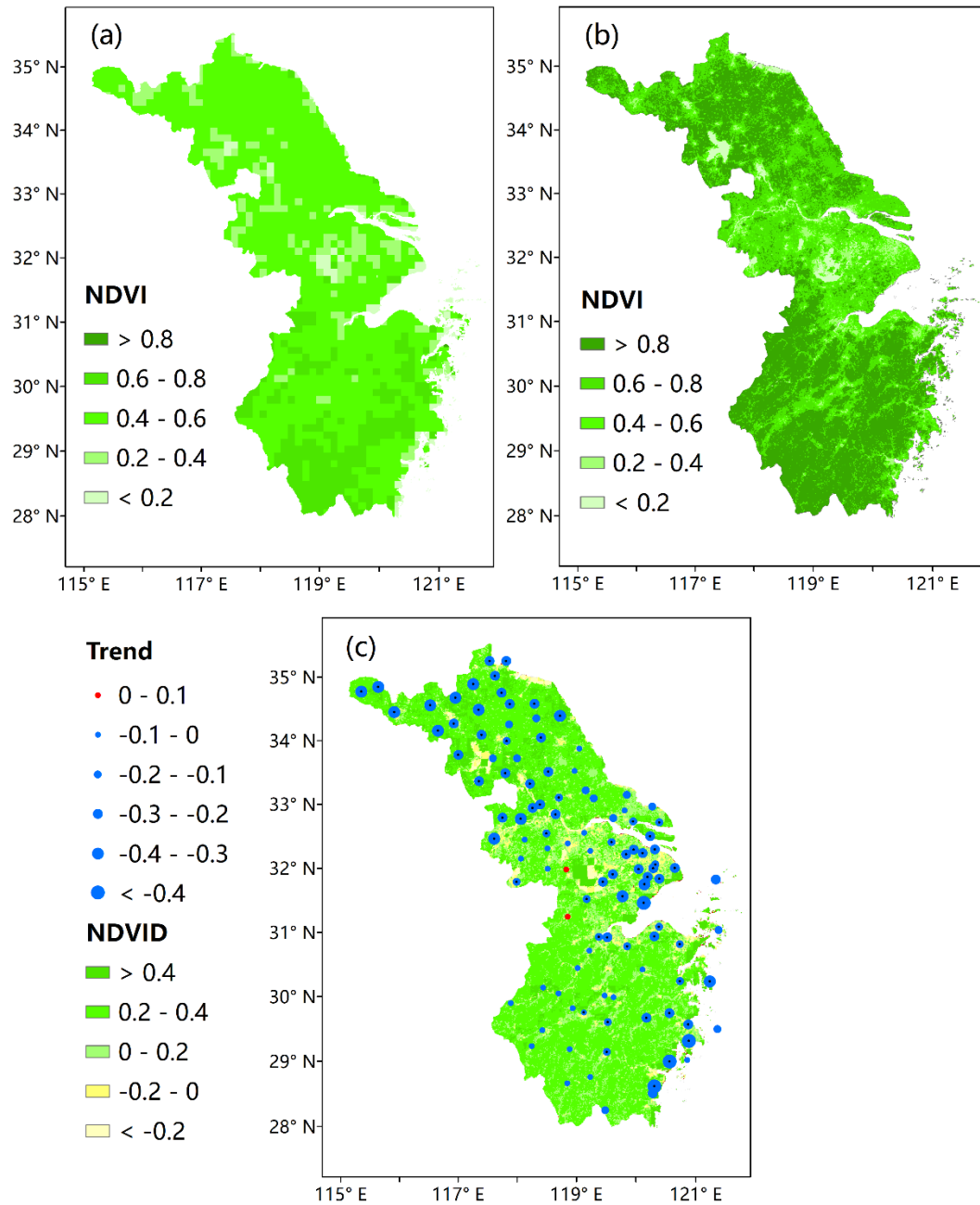


Figure 9. Distribution of NDVI (dimensionless) in (a) 1990 and (b) 2015 in the Yangtze River Delta, and (c) NDVI difference (NDVID, dimensionless) between 2015 and 1990 ((calculated as 2015 minus 1990). For the comparison with NDVID, trends (in $\text{m s}^{-1} \text{dec}^{-1}$) as well as associated significance of Daily Maximum Wind Speed (DMWS) for 1990-2015 in each of the 111 stations are also displayed. A black dot in the blue circle represents a significant trend at $p < 0.05$. The lower left legend is only for (c).